Multiperiodic orbits in a pendulum with a vertically oscillating pivot

H. J. T. Smith
Physics Department, University of Waterloo, Waterloo, Ontario, Canada

James A. Blackburn
Department of Physics and Computing, Wilfrid Laurier University, Waterloo, Ontario, Canada
(Received 26 January 1994)

Some of the complex orbits of a pendulum whose point of suspension is subjected to vertical oscillations are studied by means of an analog electronic simulator. The efficacy of this approach to problems requiring considerable interactive exploration of parameter space is demonstrated for this system. In a number of cases, confirmation of the simulator results is provided by numerical integrations of the equations of motion, together with analytic approximations. Some of the orbits have also been observed directly on an experimental realization of the vertically oscillating pendulum.

PACS number(s): 46.10.+z, 03.20.+i, 84.30.Wp

I. INTRODUCTON

Driven nonlinear systems typically exhibit extraordinarily rich dynamical modes. The most common approach to the problem of investigating these many modes is, at present, numerical simulation. The differential equations describing a system are reexpressed in some finite difference form, according to the rules of an appropriate algorithm, and the resulting algebriac problem is solved on a digital computer. Even with relatively fast desktop personal computers (PCs) and workstations, this usually turns out to be an extraordinarily slow process, involving as it does a good deal of trial-and-error searching of parameter space.

Until just a few decades ago, *analog computers* were available as commercial products. These machines were commonly employed by engineers to simulate such diverse phenomena as fluid flow, mechanical vibrations, and chemical reactions. Like the earliest digital computers, they had to be programmed by means of patch cords on large connector panels. In effect, the programmer wired together operational amplifiers, capacitors, potentiometers, switches, and other components to create a circuit which would behave as an electronic analog of the original system. These machines have now all but disappeared, victims of the digital culture. Yet the underlying rationale for analog computation remains valid, if overlooked. A properly designed circuit can often provide real-time results faster than a digital simulation on a supercomputer. Of course, there is some loss in precision—analog results might typically be valid to within a percent, whereas digital calculations can be performed to better than ten significant digits. This tradeoff of precision for speed is entirely justifiable in many cases, particularly where the original phenomenon under investigation does not lend itself in the real world to experimental verifications beyond perhaps a four or five digit accuracy. In other words, the availability of ultra precision on digital machines has led to an excessive focus on that precision. In the years since the demise of analog computers, integrated circuit op amps, integrators, differentiators, summers, multipliers, log and antilog amplifiers, etc., have undergone enormous advances in performance. As the results here will demonstrate, the analog approach using modern components can prove very effective as an analytical tool for the study of various physical phenomena.

The particular system to be considered in this paper consists of a simple pendulum whose pivot undergoes harmonic vertical displacements of specified amplitude and frequency. Certainly the most celebrated behavior of this pendulum is the possible stabilization of the "inverted" state [1–5]. This process of dynamic stabilization is of particular current interest because it is central to the operation of the Paul trap [6,7]—a charged particle confinement scheme in three dimensions which uses ac electric quadrupole fields.

In this study, we employ an electronic analog of the physical system. The observations from this simulator are then supplemented when appropriate with measurements taken from an experimental apparatus [8] consisting of a small pendulum mounted on a vertically oscillating platform, with numerical simulation data, and with analytical approximations.

For this driven pendulum, it may happen that an integer number (n_1) of pendulum oscillations occurs in a time interval during which the vertical oscillations have executed another integer number (n_2) of complete cycles. If n_1 and n_2 are either identical, or commensurate, and remain so far at least small perturbations of the system, then the pendulum has become synchronized to the forcing function. It is sometimes possible for several different *modes* of synchronization (combinations of n_1 and n_2) to be attained for the same set of parameters. The investigation of some of these characteristic synchronization modes using analog computation (electronic simulation) is the primary objective of this study. We note in passing that synchronization can also occur between autonomous oscillators subject to some degree of interactive coupling. An early description of this phenomenon was given by

Huygens [9] who discovered that two pendulum clocks attached to a common beam (which introduced a weak coupling between the pendula) ultimately would run at the same rate. Blekhman [10] and Berge [11] have written comprehensive reviews of synchronization.

II. THEORY

Consider an apparatus consisting of simple pendulum of mass m and length l, attached to a supporting structure of mass M, all of which is driven up and down by an applied force. The equation of motion of the pendulum in terms of its angular coordinate θ is then

$$-\frac{ml(F_a - mg\cos^2\theta)\sin(\theta)}{M} = I\frac{d^2\theta}{dt^2} + b\frac{d\theta}{dt}\ , \qquad (1)$$

where I is the moment of inertia of the pendulum, b is the velocity dependent damping coefficient, and F_a is the total vertical force that is applied to the mass M. In practice it is the position, rather than the force, which is defined by the drive. For the case of a sinusoidal displacement (at frequency ω), F_a is given by

$$F_a = Mg + mg\cos^2\theta - F_0\cos(\omega t)\ . \qquad (2)$$

In most practical situations $M > m$. Combining Eqs. (1) and (2) and using the following identities,

$$F_0 = MA\omega^2,\quad \Omega = \frac{\omega}{\omega_0},\quad Q = I\frac{\omega_0}{b},$$

$$\epsilon = \frac{A}{l},\quad \tau = \omega_0 t,\quad \omega_0 = \left[\frac{g}{l}\right]^{1/2},$$

where A is the amplitude of the displacement of the mass M and τ is dimensionless time, gives the normalized equation of motion of the system:

$$\frac{d^2\theta}{d\tau^2} + \frac{1}{Q}\frac{d\theta}{d\tau} + [1 - \epsilon\Omega^2\cos(\Omega\tau)]\sin(\theta) = 0\ . \qquad (3)$$

In the zero damping limit and for small-angle motion about the vertical equilibrium position, this becomes the Mathieu equation for which a considerable literature exists detailing in particular the various regions of stability [1–5].

A fundamental principal which must be obeyed in a steady state is the requirement that the "average" energy input to this system must equal the energy dissipated. This is not a continuous condition, but one that must be satisfied when integrated over some appropriate time interval. For this harmonically driven system, the integration must be applied over a number of complete cycles of the input excitation. In some orbits, as will be seen, the pendulum continuously rotates and so θ monotonically increases with time, although certainly not in a linear manner. For other orbits, the pendulum coordinate θ oscillates about a fixed value.

Several methodologies were employed in this study of dynamical modes of an inverted pendulum. An experimental apparatus was constructed which permitted direct observation of the motion of a "real" system. Numerical solutions of Eq. (3) were computed using a fourth order Runge-Kutta algorithm. Where appropriate, analytical approximations to the desired phase space orbits could be obtained. Finally, as noted already, we designed an electronic analog of the pendulum. This design will now be described in some detail.

III. ANALOG COMPUTATION

Figure 1(a) is a schematic of the complete electronic simulator. The sine generator, Fig. 1(b), is a voltage controlled oscillator (VCO) with an output which can be expressed in the form $V_s\sin(\theta)$ where $d\theta/dt = 2\pi K V_0$ (see Wu *et al.* [12]) and V_0 is the input to the sine generator. The amplitude V_s of the sine generator circuit was nominally targeted to be 1 V; in the actual circuit its measured value was 0.933 V. Similarly, the design goal for the constant K was 1 kHz/V; it was measured as 990 Hz/V. The angular coordinate θ is generated by that part of the VCO circuit [Fig. 1(b)] which is enclosed by the dashed box. Note that the circuit sets the angle in the range $-\pi/2 > \theta > 3\pi/2$. In Fig. 1(a), the leftmost op amp performs the current summation,

$$C_1\frac{dV_0}{dt} + \frac{V_0}{R_3} + \frac{V_s\sin(\theta)}{R_2} + \frac{V_i\sin(\omega t)V_s\sin(\theta)}{(10)R_1} = 0\ , \qquad (4)$$

which reduces to

$$C_1\frac{d^2\theta}{dt^2} + \frac{1}{R_3}\frac{d\theta}{dt} + 2\pi K\left[\frac{1}{R_2} + \frac{V_i\sin(\omega t)}{(10)R_1}\right]V_s\sin(\theta) = 0\ , \qquad (5)$$

where the output of the op amp is V_0. Also note that the electronic multipliers (Analog Devices: AD532) have a built-in divide-by-10 feature. Initial conditions are set in the conventional way by precharging the appropriate integrating capacitors. $(d\theta/dt)_i$ is set by precharging C_1 by means of the battery and switch, while θ_i is set by precharging the capacitor of the integrator in the sine generator circuit [Fig. 1(b)], again using a potential source and switch.

The natural frequency ω_0, with $V_i = 0$ is given by

$$\omega_0 = \left[\frac{2\pi K V_s}{R_2 C_1}\right]^{1/2}.$$

Equations (3) (the pendulum) and (5) (the analog circuit) can be made equivalent by normalizing time to $1/\omega_0$ and by using the following identities:

$$Q = C_1 R_3\omega_0,\quad \epsilon = \frac{V_i R_2\omega_0^2}{\omega^2 R_1(10)},\quad \Omega = \frac{\omega}{\omega_0},\quad \frac{d\theta}{d\tau} = \frac{V_0 2\pi K}{\omega_0}\ .$$

The X and Y position coordinates of the pendulum bob are electronically generated by the multiplier and integrator in the dashed box of Fig. 1(a), as can be seen from the following discussion. Note first that the output of the integrator is

$$\frac{-1}{R_4C_2(10)}\int_0^t V_0V_s\sin(\theta)dt\ .$$

But $d\theta/dt=2\pi KV_0$ and by setting $R_4C_2(10)=(2\pi K)^{-1}$ (that is $C_2=0.0047$ μF and $R_4=3420$ Ω in the present case) this output becomes exactly $V_s\cos(\theta)$. In real space units, the horizontal and vertical coordinates of the pendulum bob are $l\sin(\theta)$ and $l[\cos(\theta)+\epsilon\cos(\omega t)]$, respectively. The analog voltage equivalents of these coordinates, as indicated in Fig. 1(a), are $V_s\sin(\theta)$ and $[V_s\cos(\theta)+V_i(R_5/R_6)\sin(\omega t)]$. Hence the simulated true space motion of the pendulum bob can be viewed directly on an oscilloscope by simply feeding these two voltages to the x and y inputs. Note that $R_5/R_6=V_sR_2/(R_1\Omega^2 10)$ so that R_5 and/or R_6 must be set to new values for each choice of excitation frequency Ω.

Thus the electronic analog simulator provides both a phase plot and a coordinate plot. The values of C_1 and R_2 are chosen so that ω_0 is within the operating frequency range (10–10 000 Hz) of the op amps. For the experiments reported here, ω_0 was set equal to 779 rad/s ($f_0=124$ Hz) by making $C_1=0.097$ μF and $R_2=99.1$ kohm. The *measured* low amplitude natural frequency was 760 rad/s ($f_0=121$ Hz). By setting $R_3=280.5$ kohm, a design target of Q equal to 22 was established;

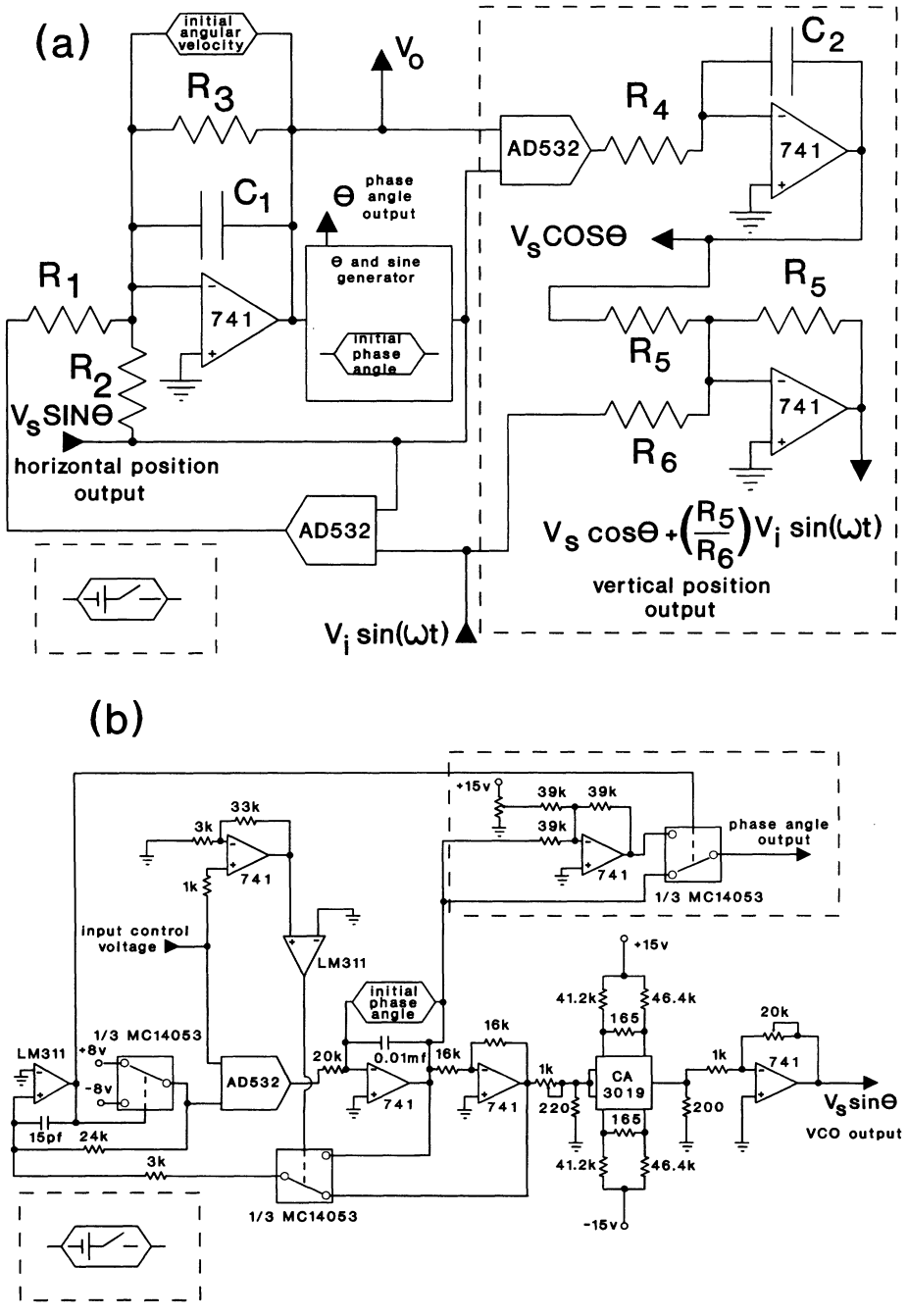

FIG. 1. (a) Schematic of the electronic analog simulator. The op amps are 741's and the analog multipliers are type AD532 from Analog Devices. (b) Schematic of the voltage controlled oscillator and sine generator.

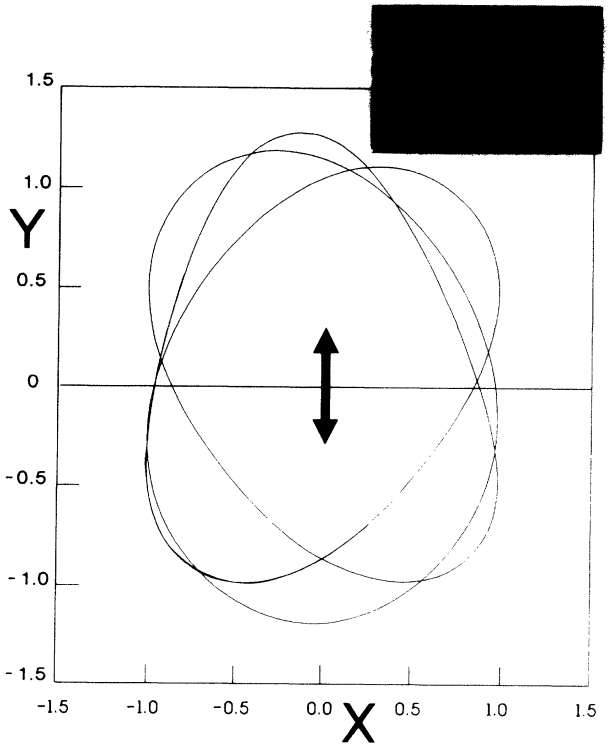

FIG. 2. A plot of an $n_1=1$, $n_2=3$ trajectory of the pendulum mass from the analog simulator with parameters $Q=22$, $\epsilon=0.30$, and $\Omega=6.5$. The inset is a photograph taken directly from an oscilloscope display of the simulator output. The X and Y dimensions are in units of l. The arrow indicates the extent of travel of the pivot.

the *measured* value of Q was 19.

The possible periodic orbits for this system have been divided into two groups: (i) rotational orbits in which θ increases monotonically with time (steady phase winding) and (ii) oscillating orbits where θ fluctuates about some fixed reference phase. The vertically up ($\uparrow$) and vertically down ($\downarrow$) modes fall within this latter category. The pendulum coordinate $\theta(t)$ is repetitive, completing n_1 cycles in an interval within which there are n_2 cycles of the drive signal. The integers n_1 and n_2 thus serve to label the periodic orbits.

To facilitate subsequent analysis of the pendulum motion, the analog outputs (X, Y) from the electronic simulator were digitized in real time with a Keithley MetraByte DAS20 PC data acquisition board.

IV. ROTATIONAL MULTIPERIODIC ORBITS

Rotational multiperiodic orbits with $n_1=1$ and $n_2=1$, 2 or 3 synchronizations are easily detectable. The difference (δ) between angle θ and the drive phase $\Omega\tau$ is a particularly useful indicator of orbit type. With the definition $\delta(\tau)=[\theta(\tau)-\Omega\tau]-\pi$, Eq. (3) becomes

$$\frac{d^2\delta}{d\tau^2}+\frac{\Omega}{Q}+\frac{1}{Q}\frac{d\delta}{d\tau}+[1-\epsilon\Omega^2\cos(\Omega\tau)]\sin(\Omega\tau+\delta+\pi)=0\ , \quad (6)$$

which can also be expressed

$$\frac{d^2\delta}{d\tau^2}+\frac{\Omega}{Q}+\frac{1}{Q}\frac{d\delta}{d\tau}+\sin(\Omega\tau+\delta+\pi)=\frac{\epsilon\Omega^2}{2}[\sin(2\Omega\tau+\delta+\pi)+\sin(\delta+\pi)]\ . \quad (7)$$

FIG. 3. A photograph of the actual pendulum in a rotational multiperiodic orbit $n_1=1$, $n_2=3$ with the pendulum parameters estimated to be $Q=22$, $\epsilon=0.30$, and $\Omega=6.55$—that is, essentially the same as for the previous figure.

Example: $n_1=1$, $n_2=3$. Parameters for the electronic simulator were set to $Q=22$, $\epsilon=0.30$, and $\Omega=6.5$. The resulting simulated motion of the tip of the pendulum is shown in Fig. 2, where the inset is a photograph taken directly from the oscilloscope and the larger drawing is constructed from digitized data.

This mode was also observed with the experimental apparatus [8], as can be seen in Fig. 3, for which the parameter values were $Q=22$, $\epsilon=0.30$, and $\Omega=6.55$. The image of the illuminated pendulum was projected directly onto a sheet of 8×10 standard photographic paper using a 75-mm, f1.9 lens. This method of direct projection results in a negative image of the apparatus.

Figure 4 is a corresponding plot obtained from a numerical solution of Eq. (3), again with the same parameters. There is close agreement with both analog simulation and experiment. It was found that this particular orbit could be obtained only for a limited range of initial conditions. This does not pose a problem for numerical simulations, but experimentally such is not the case. In practice, the pendulum was started with a number of different initial conditions until the required orbit was obtained.

From the point of view of analytical approximations, it must first be noted that the pendulum is rotating, and so

$$\delta\approx\delta_c+\delta_0\sin(\Omega\tau+\phi)\ . \tag{8}$$

With the amplitude of the oscillations of δ large, as is true in this example, δ can be approximated as $\delta\approx\delta_0\sin(\Omega\tau+\phi)$. There are some harmonics at frequency 2Ω in $\delta(\tau)$ which balance the $\sin(2\Omega\tau+\delta)$ term on the right of Eq. (7). Thus by assuming that δ contains no harmonics in 2Ω, then the $\sin(2\Omega\tau+\delta+\pi)$ term in Eq. (7) can be ignored. Hence

$$\frac{d^2\delta}{d\tau^2}+\frac{1}{Q}\frac{d\delta}{d\tau}+\frac{\epsilon\Omega^2}{2}\sin(\delta)=-\frac{\Omega}{Q}+\sin(\theta)\ , \tag{9}$$

which has the form of an equation of a driven damped "pendulum" with angular "coordinate" δ. The frequency of large-amplitude (maximum displacement δ_0) natural oscillations of an undamped pseudo pendulum, represented by Eq. (9) in the limit $Q\to\infty$, can be expressed as

$$\frac{n_1}{n_2}\Omega=\left[\frac{\epsilon\Omega^2}{2}\right]^{1/2}\left[\frac{2}{\pi}K(\sin(\delta_0/2))\right]^{-1}\ , \tag{10}$$

where $(n_1/n_2)\Omega$ is the resonant frequency and K is a complete elliptic integral of the first kind. Equation (3) was numerically solved with appropriate values of Q, Ω, and ϵ in order to obtain various rotational synchronous modes. In Table I, values of δ_0 from the numerical simulations are compared to values calculated from Eq. (10).

TABLE I. A comparison of values of δ_0 from a numerical calculation of Eq. (3) and from the formula Eq. (10) using $Q=22$.

n_1	n_2	ϵ	Ω	δ_0 [Eq. (10)]	δ_0 [Eq. (3)]
1	3	0.25	4.1	0.95	1.1
1	3	0.30	5	1.51	1.45
1	3	0.35	7	1.82	1.85
1	3	0.38	10	1.96	2.0
2	5	0.38	15	1.20	1.2
1	4	0.16	3	1.37	1.4
1	2	0.60	15	1.19	1.2

The effective drive term $\sin(\theta)$ on the right hand side of Eq. (9) contains many harmonics. For the undulations in the rotational motion to become synchronized to the drive signal, a harmonic of $\sin(\theta)$ must correspond to the frequency of oscillation of the pseudopendulum, which itself is a function of its amplitude δ_0. This amplitude will

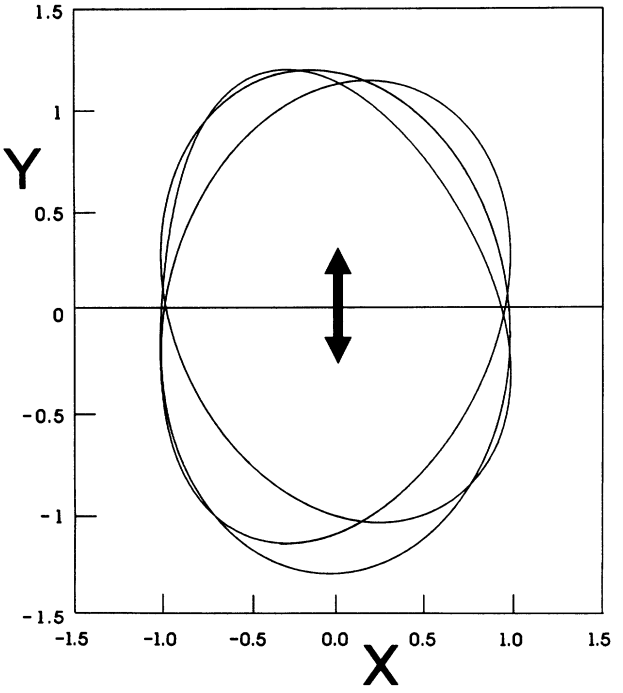

FIG. 4. The calculated trajectory (numerical integration) of the tip of the pendulum for the parameters of Fig. 3 using the initial conditions $\theta_i=1.526$ rad and $(d\theta/d\tau)_i=4.861$. The X and Y dimensions are in units of l. The arrow indicates the extent of travel of the pivot.

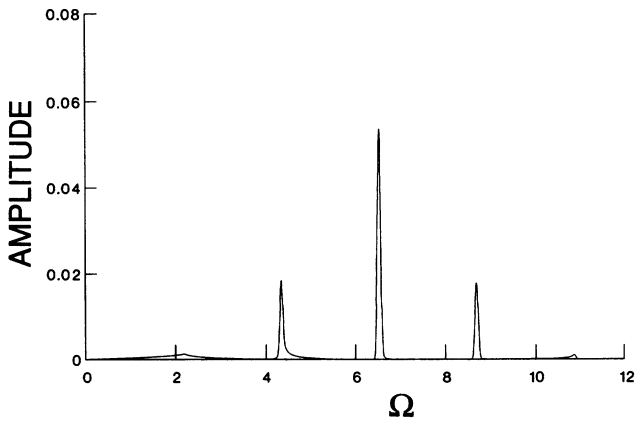

FIG. 5. Power spectrum of the pendulum (numerical simulations) in the rotational multiperiodic orbit $n_1=1$, $n_2=3$ with parameters $\epsilon=0.25$, $Q=22$, and $\Omega=6.5$.

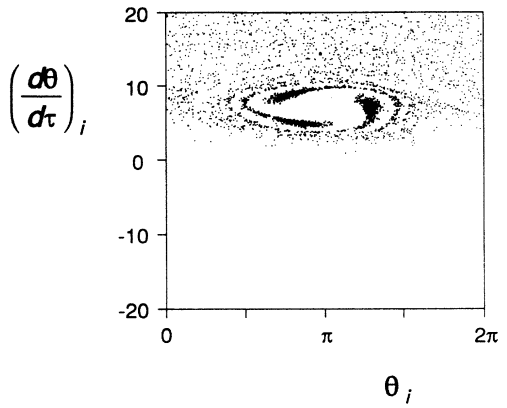

FIG. 6. Basin of attraction for the mode depicted in Fig. 5.

adjust until the oscillation frequency is equal to a harmonic of $\sin(\theta)$. However, the amplitude of δ_0 is restricted to the range of 0 to π. When $\delta_0=\pi$ the oscillation frequency would be zero. Thus whether or not synchronization occurs is dependent on the harmonic content of $\sin(\theta)$.

This issue was investigated using the specific mode $n_1=1$, $n_2=3$ in part because it can be achieved over a wide range of the parameters ϵ, Ω, and Q. Equation (3) was solved numerically for ($Q=22$, $\epsilon=0.25$, $\Omega=6.5$) and the power spectrum of the resulting time series $\theta(t)$ was calculated.

An inspection of Eq. (10) reveals that with the parame-

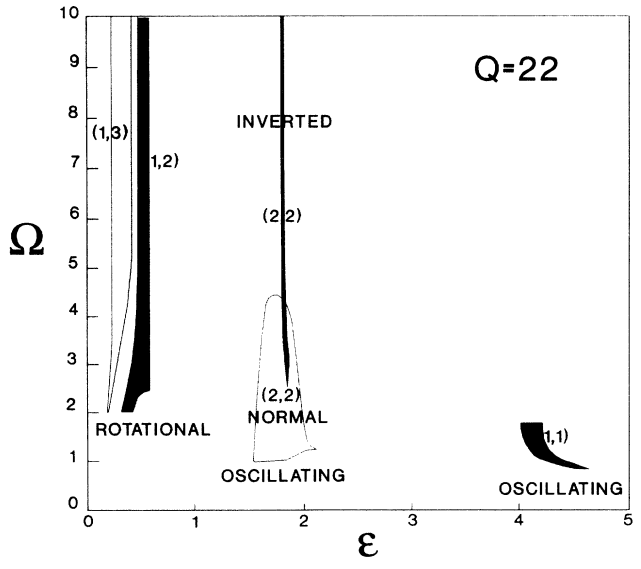

FIG. 7. A state diagram showing the values of Ω and ϵ (for $Q=22$) which lead to $n_1=1$, $n_2=2$ (dark shading) and $n_1=1$, $n_2=3$ (light shading) rotating orbits. The domains of several other oscillating modes are also indicated. Rotating modes cannot occur to the left of a boundary line that is given by $\epsilon=2[\Omega Q]^{-1}$. The (1,1) rotating mode can occur in all nonshaded regions for $\Omega>2$. Not all possible modes are shown in this figure. For example, the (4,4) mode is a bifurcation of the (2,2) mode and occurs in a very small region to the right of the shaded patch for the (2,2) state.

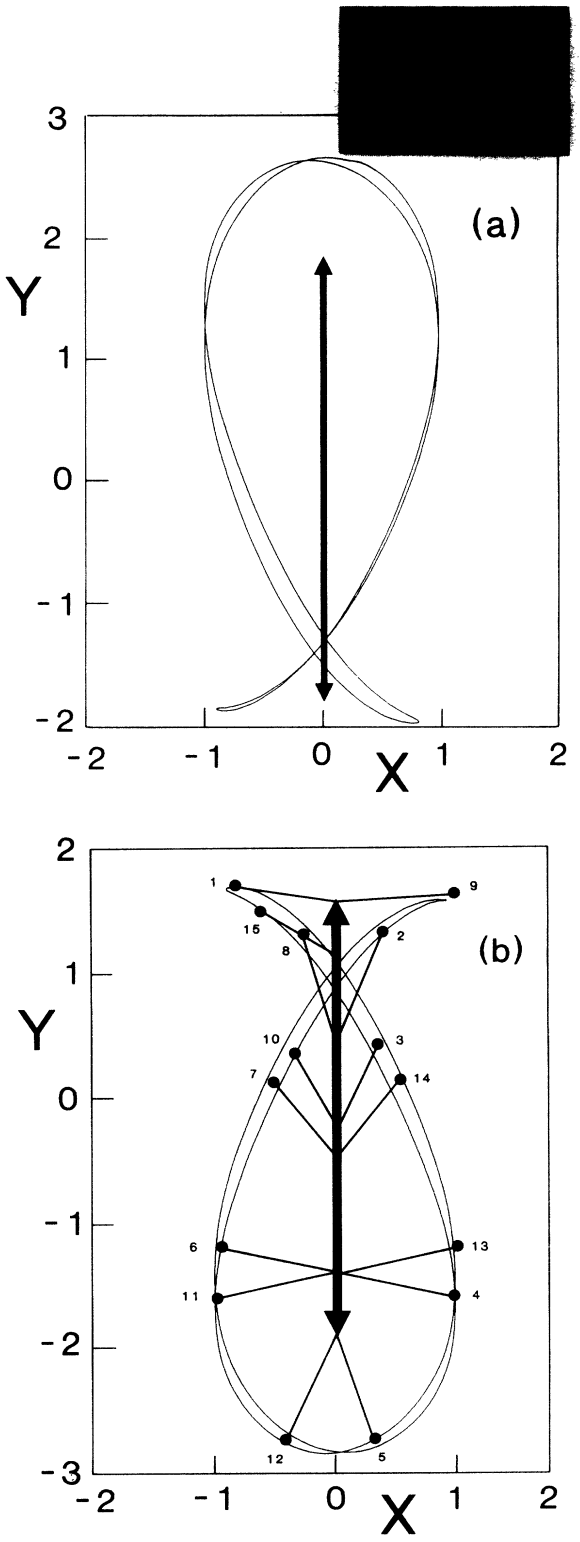

FIG. 8. The space trajectory of the tip of the pendulum, from the electronic analog simulator, for $\Omega=3.38$, $Q=22$, and $\epsilon=1.84$ showing the $n_1=2$, $n_2=2$ oscillating orbit. (a) Normal (the inset is a photograph taken directly from an oscilloscope display of the simulator output; (b) inverted. The X and Y dimensions are in units of l. The arrow indicates the extent of travel of the pivot and the approximate position of the pendulum has been sketched in to show the motion.

ters ($Q=22$, $\epsilon=0.25$, $\Omega=6.5$), the factor $(n_1/n_2)\Omega$ must be between 3.6 and 0 in order for δ_0 to bet between 0 and π. In Fig. 5 (the power spectrum), the only harmonic of $\sin(\theta)$ in this range is at $\Omega=2.167$. Although it has a small amplitude, it is still strong enough to drive the pseudopendulum. Of course there are competing orbits, principally the $n_1=1$, $n_2=1$ rotational mode.

The basin of attraction for this $n_1=1$, $n_2=3$ mode was also obtained for the parameters ($Q=22$, $\epsilon=0.25$, $\Omega=6.5$) using interpolated cell mapping [13–16]. This basin, plotted in Fig. 6, indicates the domain of initial conditions which lead ultimately to this orbit.

The example just given illustrates the constructive interplay among the three methods being applied to this problem: electronic simulation, direct experimentation, and numerical computation. Other modes such as $n_1=1$, $n_2=1$ and $n_1=1$, $n_2=2$ were also observed. The approximate domains in parameter space $[\epsilon,\Omega]$ of these rotational modes are indicated in Fig. 7. Comparison with Fig. 4 of Ref. [5] reveals that these domains are coexistent with stability regions for the normal and inverted states of the pendulum.

V. OSCILLATING PERIODIC ORBITS

In these modes the pendulum executes oscillations about some constant angle. The amplitude of these oscillations will depend upon the particular orbit and it may be small or large, even greater than 2π in some cases. The vertically up (inverted state) and vertically down (normal state) orbits are examples where the amplitude is small.

Example: $n_1=2$, $n_2=2$. The $n_1=2$, $n_2=2$ orbit is especially interesting because the amplitude of oscillation is greater than 2π. The pendulum alternately rotates in one direction and then reverses for more than 2π rad but less than 3π rad. One cycle of the drive force is required to complete the forward rotation of the pendulum and a second cycle of the drive force is needed to complete the reverse rotation.

Figures 8(a) and 8(b) show two trajectories of the pendulum as observed on the electronic analog simulator for $Q=22$, $\epsilon=1.84$, and $\Omega=3.38$. Note that one is the inversion of the other. For convenience we have labeled the orbit of Fig. 8(a) as the "normal" orbit and that of Fig. 8(b) the inverted orbit. The approximate position of the pendulum has been sketched in a numbered sequence in order to show the motion.

The domain of the $n_1=2$, $n_2=2$ orbit in parameter space $[\Omega,\epsilon]$ is indicated in Fig. 7. It is subdivided into darkly shaded region in which the final state is reached relatively quickly with the indicated parameter values, and a lightly shaded region in which a lengthy interval of transient chaos [17–20] precedes the arrival at the final state. These transient times can be as long as thousands of periods of the driving force. Many other oscillating modes were observed, including $n_1=1$, $n_2=1$ and $n_1=1$, $n_2=4$.

VI. CONCLUSIONS

Some of the multiperiodic orbits of the pivot driven pendulum have been described and their domains in state space are determined by means of an electronic analog of the nonlinear system. It is worth noting that the richness of modes in this system complicates the task of exploring its salient features, and serves to underscore the significant advantages of high speed analog computation for this type of problem.

ACKNOWLEDGMENT

This work was supported in part by grants from the Natural Sciences and Engineering Council of Canada.

[1] M. M. Michaelis, Am. J. Phys. **53**, 1079 (1985).
[2] D. J. Ness, Am. J. Phys. **35**, 964 (1967).
[3] F. M. Phelps III and J. H. Hunter, Jr., Am. J. Phys. **33**, 285 (1965).
[4] J. J. Stoker, *Nonlinear Vibrations in Mechanical and Electrical Systems* (Wiley, New York, 1966), pp. 202–213.
[5] J. A. Blackburn, H. J. T. Smith, and N. Grønbech-Jensen, Am. J. Phys. **60**, 903 (1992).
[6] H. Winter and H. W. Ortjohann, Am. J. Phys. **59**, 807 (1991).
[7] J. Hoffnagle and R. G. Brewer, Phys. Rev. Lett. **71**, 1828 (1993).
[8] H. J. T. Smith and J. A. Blackburn, Am. J. Phys. **60**, 909 (1992).
[9] C. Huygens, *Oeuvres Completes des Christian Huyghens,* edited by M. Nijhoff (Societé Hollandaise des Sciences, The Hague, The Netherlands, 1893), Vol. 5, p. 243.
[10] I. I. Blekhman, *Synchronization in Science and Technology,* ASME Press translations (American Society of Mechanical Engineers, New York, 1988).
[11] P. Berge, Y. Pomeau, and C. Vidal, *Order within Chaos* (Hermann, Paris, 1984), p. 289.
[12] B. Wu, Yang Zhou-jing, J. A. Blackburn, S. Vik, H. J. T. Smith, and M. A. H. Nerenberg, Phys. Rev. B **37**, 3349 (1988).
[13] C. S. Hsu, J. Appl. Mech. **47**, 931 (1980).
[14] C. S. Hsu and R. S. Guttalu, Trans. Am. Soc. Mech. Eng. **47**, 940 (1980).
[15] B. H. Tongue, Physica D **28**, 401 (1987).
[16] B. H. Tongue and K. Gu, SIAM (Soc. Ind. Appl. Math.) J. Appl. Math. **48**, 1206 (1988).
[17] B. P. Koch and R. W. Leven, Physica D **16**, 1 (1985).
[18] R. W. Leven and B. P. Koch, Phys. Lett. A **86**, 71 (1981).
[19] B. P. Koch, R. W. Leven, B. Pompe, and C. Wilke, Phys. Lett. A **96**, 219 (1983).
[20] R. W. Leven, B. Pompe, C. Wilke, and B. P. Koch, Physica D **16**, 371 (1985).

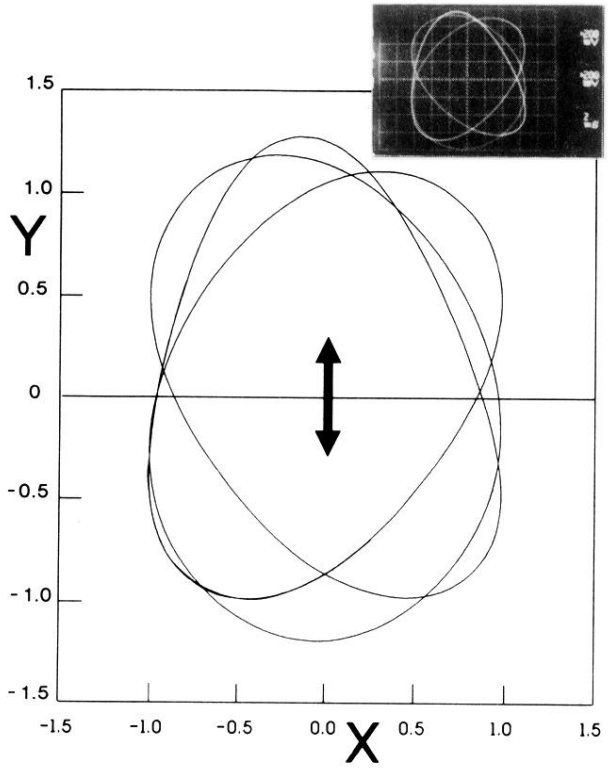

FIG. 2. A plot of an $n_1=1$, $n_2=3$ trajectory of the pendulum mass from the analog simulator with parameters $Q=22$, $\epsilon=0.30$, and $\Omega=6.5$. The inset is a photograph taken directly from an oscilloscope display of the simulator output. The X and Y dimensions are in units of l. The arrow indicates the extent of travel of the pivot.

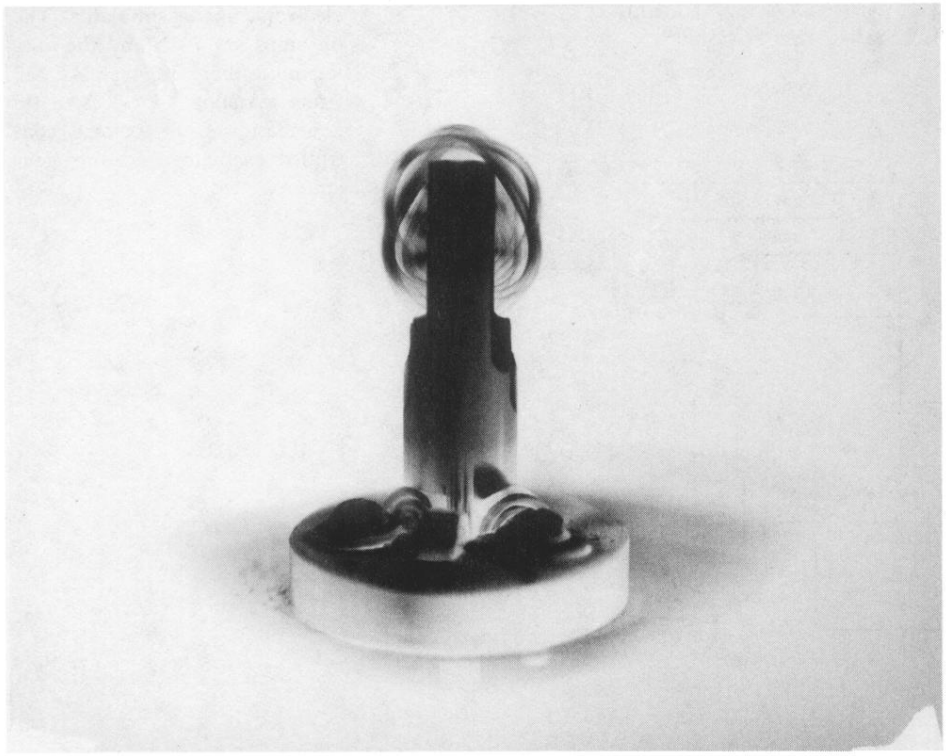

FIG. 3. A photograph of the actual pendulum in a rotational multiperiodic orbit $n_1=1$, $n_2=3$ with the pendulum parameters estimated to be $Q=22$, $\epsilon=0.30$, and $\Omega=6.55$—that is, essentially the same as for the previous figure.

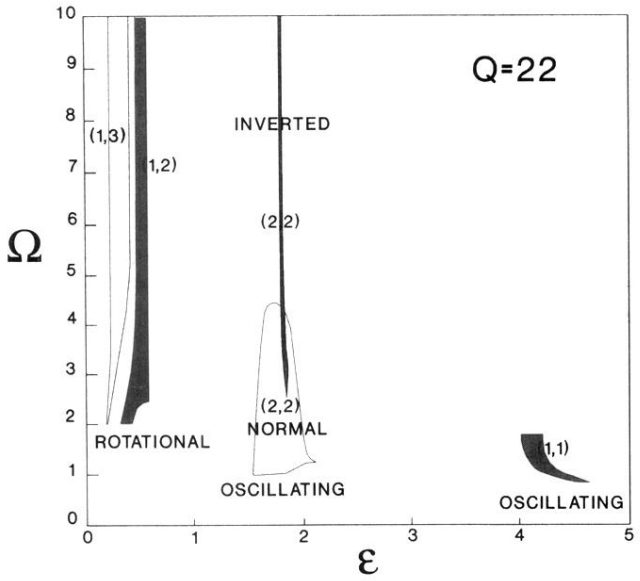

FIG. 7. A state diagram showing the values of Ω and ϵ (for $Q=22$) which lead to $n_1=1$, $n_2=2$ (dark shading) and $n_1=1$, $n_2=3$ (light shading) rotating orbits. The domains of several other oscillating modes are also indicated. Rotating modes cannot occur to the left of a boundary line that is given by $\epsilon=2[\Omega Q]^{-1}$. The (1,1) rotating mode can occur in all nonshaded regions for $\Omega>2$. Not all possible modes are shown in this figure. For example, the (4,4) mode is a bifurcation of the (2,2) mode and occurs in a very small region to the right of the shaded patch for the (2,2) state.

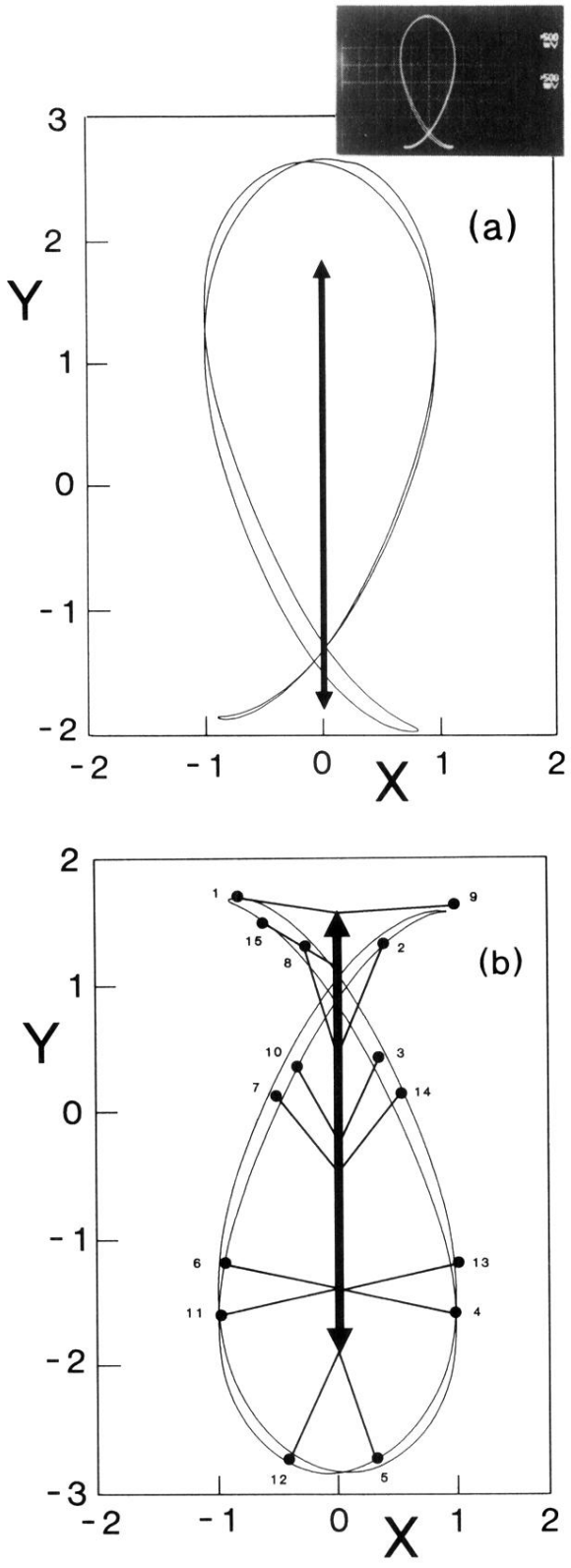

FIG. 8. The space trajectory of the tip of the pendulum, from the electronic analog simulator, for $\Omega=3.38$, $Q=22$, and $\epsilon=1.84$ showing the $n_1=2$, $n_2=2$ oscillating orbit. (a) Normal (the inset is a photograph taken directly from an oscilloscope display of the simulator output; (b) inverted. The X and Y dimensions are in units of l. The arrow indicates the extent of travel of the pivot and the approximate position of the pendulum has been sketched in to show the motion.